

## WHAT IS THE ROLE OF THE STAGNATION REGION IN KARMAN VORTEX SHEDDING?

**Grzegorz L. Pankanin**

*Institute of Electronic Systems, Warsaw University of Technology, ul. Nowowiejska 15/19, 00-665 Warsaw, Poland  
(✉g.pankanin@ise.pw.edu.pl)*

### Abstract

This paper is devoted to the problem of the appearance of a stagnation region during Karman vortex shedding. This particular phenomenon has been addressed by G. Birkhoff in his model of vortices generation. Experimental results obtained by various research methods confirm the existence of a stagnation region. The properties of this stagnation region have been described based on experimental findings involving flow visualisation and hot-wire anemometry. Special attention has been paid to the relationship between the existence of a slit in the bluff body and the size of the stagnation region. The slit takes over the role of the stagnation region as an information channel for generating vortices.

Keywords: flow measurement, Karman vortex shedding, bluff body, stagnation region.

© 2011 Polish Academy of Sciences. All rights reserved

### 1. Introduction

The well-known vortex meter is based on the generation of the Karman vortex street on an obstacle placed in the flowing fluid. Numerous articles and papers are devoted to this subject [1]. Most of them, however, concern only very narrow and selected problems: the bluff body shape [2-6], sensor type [7-9] or signal processing systems [10-14]. However, the phenomena accompanying the vortex shedding are more complicated than they initially seem. As vortex meter designers know very well, even small structural details may strongly influence the vortex shedding. Therefore, investigations leading to comprehensive understanding of the phenomena are necessary.



Fig. 1. Stagnation region.

Stagnation region appearance (Fig. 1) during vortex shedding is seldom discussed. In this article, analyses and investigations of this effect are aimed at discovering its influence on vortex shedding.

The stagnation region originally appeared in Birkhoff's model of vortex shedding [15-17]. G. Birkhoff assumed that a certain volume of fluid clustered downstream of the bluff body performs the push-pull motion associated with vortex shedding. Understanding the role of the stagnation region in vortex shedding is a key factor in recognition of the Karman vortex street phenomenon.

## 2. Karman vortex shedding

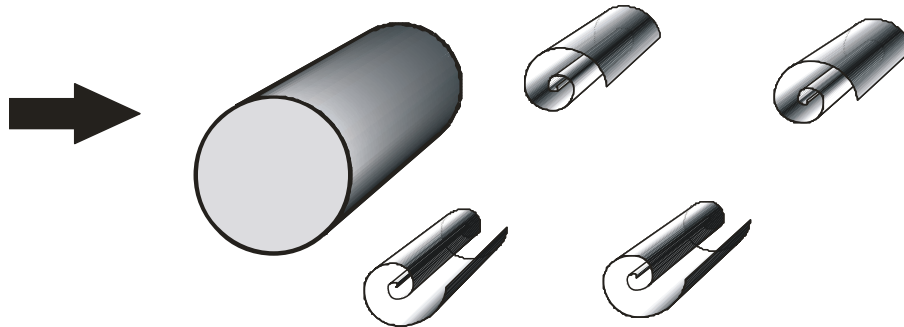


Fig. 2. Karman vortex shedding.

The vortex flow meter is based on the phenomenon of Karman vortex shedding on an obstacle placed in the flowing fluid (Fig. 2). The frequency of vortices shedding alternatively on both sides of the bluff body is a linear function of the flow velocity:

$$f = S_T \cdot \frac{v}{d}. \quad (1)$$

The Strouhal number,  $S_T$ , is constant over a very wide range of flow velocities and is independent of the physical properties of the fluid. Therefore, the flow meter is not sensitive to the temperature, viscosity or density of the medium. Moreover, the same flow-rate measurements are obtained for gas and for liquid.

Concerning the flow measurement, the strength and regularity of the generated vortices are of the greatest importance [1]. This finding is based on the results of previous investigations carried out by various researchers, which have revealed that the energy and regularity of the vortices mainly depends on the shape and dimensions of the bluff body [2, 5, 6, 18].

It should also be noted that several poorly-defined factors may influence the phenomenon. As seen in Fig. 1, the vortex shedding on the obstacle is accompanied by characteristic fluid behaviour in the closest neighbourhood downstream of the bluff body. This area of limited fluid movement alone is the subject of this paper, and its role in vortex shedding is discussed.

## 3. Birkhoff's model

Birkhoff proposed [15-17] his model of vortex generation as an oscillating "fishtail" (Fig. 3). This model is based on an assumption of the appearance of a low-motion area nearby, just downstream from the bluff body. The fluid in the region does not move along the pipe axis but performs the oscillating movement, relaying information on the generated vortex to the other side of the bluff body.

Birkhoff analysed the phenomena accompanying vortex shedding on a circular cylinder of diameter  $d$  and unitary length  $L$ . It was assumed that the stagnation region is of dimensions  $h$

and  $2L$  and that its centre of gravity  $G$  performs oscillating movements around the bluff body axis (Fig. 3).

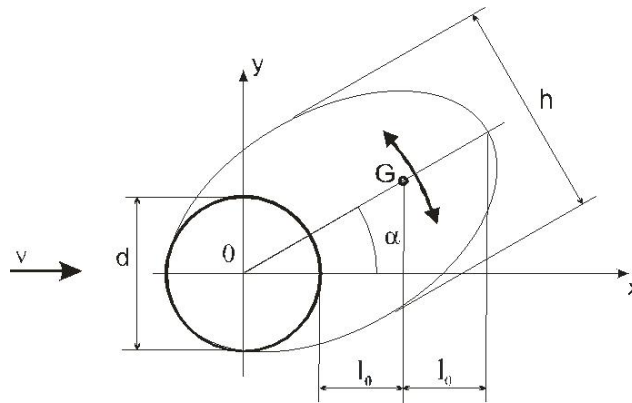


Fig. 3. Birkhoff's model (after: Funakawa [17] and Cousins [19]).

The equation describing the oscillations of this physical arrangement is as follows [17]:

$$I \cdot \frac{d^2 \alpha}{dt^2} + k_r \cdot \alpha = 0, \quad (2)$$

where the moment of inertia is given by [17]:

$$I = 2 \cdot \rho \cdot h \cdot l_0 \cdot \left(\frac{d}{2} + l_0\right)^2 \quad (3)$$

and the coefficient of the restoring moment acting on the "fishtail" is given by [17]:

$$k_r = 2\pi \cdot \rho \cdot v^2 \cdot \left(\frac{d}{2} + l_0\right) \cdot l_0. \quad (4)$$

By substituting (3) and (4) into (2) and solving the differential equation, the following expression is obtained [17]:

$$f = \frac{v}{\sqrt{4 \cdot \pi \cdot h \cdot \left(\frac{d}{2} + l_0\right)}}. \quad (5)$$

Based on (5), the frequency of generated vortices is directly proportional to the flow velocity and does not depend on the fluid density or the Reynolds number.

Therefore, the Strouhal number can be expressed as follows [17]:

$$S_T = \frac{f \cdot d}{v} = \frac{d}{\sqrt{4 \cdot \pi \cdot h \cdot \left(\frac{d}{2} + l_0\right)}}. \quad (6)$$

Assuming that  $h = 1.25 \cdot d$  and  $l_0 = 1.1 \cdot d$  (experimentally verified by Funakawa [17]), the calculated Strouhal number reaches  $S_T = 0.2$ . This value is close to the values obtained experimentally.

#### 4. The stagnation region in the phenomenological model

The phenomenological model of the vortex development, described in detail in [20], has been worked out by the team managed by the author of the paper. Its conception is based on laboratory investigations of the phenomenon and on literature analyses. The stagnation region appearance alone matters greatly in the model foundations.

By simulating the vortex development using the phenomenological model, the changeability of the vortex rotation energy as a function of the current vortex location can be found (Fig. 4) [21]. After intensive energy growth, a gradual (depending on the fluid viscosity) energy decrease is observed.

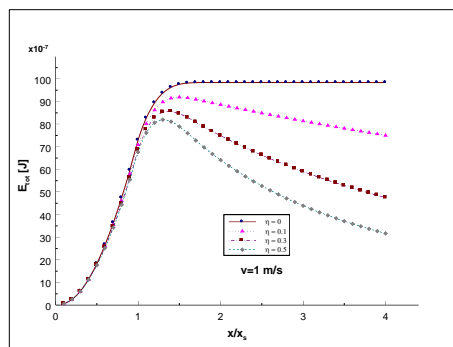


Fig. 4. Total rotation energy of the vortex as a function of the current vortex location [21].

Considering the subject of this paper, the influence of the length of the stagnation region on the rotation energy may be interesting (Fig. 5).

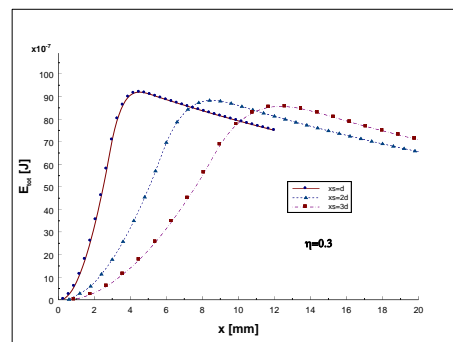


Fig. 5. Rotation energy vs. vortex location for various stagnation region lengths ( $x_s$  – stagnation region length,  $d$  – bluff body diameter) [22].

As seen, the stagnation region length considerably influences the rate of the vortex rotational energy growth. A shorter stagnation region forces more intensive vortex development and the maximum energy appears closer the bluff body. This observation is also of great importance when considering the optimal sensor location. However, the most important conclusion is that the stagnation region is a critical factor that influences the vortex development.

## 5. Laboratory investigations confirming the existence of the stagnation region

When formulating any model of the considered phenomena, laboratory verification of assumptions in the proposed model is crucial. Therefore, practical confirmation of the stagnation region is of key importance.

In laboratory investigations, stagnation region behavior in various circumstances can be observed. Using various research methods, it is possible to get valuable results concerning the investigated phenomena.

### 5.1. Flow visualization

Flow visualization is a very useful method for investigating fluid mechanics. Many discoveries in this field were supported by flow visualization. From the very beginning, the Karman vortex street phenomenon has been investigated using flow visualization [5, 23, 24].

Flow visualization enables observation of the entire flow area at the same moment. Therefore, in the case of Karman vortex street, not only the vortices but also the accompanying effects can be analyzed. The appearance of the stagnation region, the subject of this paper, is an example of such an effect.

Due to the rapid development of fast cameras, new abilities to investigate these phenomena have appeared. Analyzing consecutive pictures of the phenomenon, the convection velocity of the Karman vortices can be calculated. Thanks to the application of this method, the previously unknown effect of its changeability has been discovered [25, 26].

The flow visualization experiments were carried out on a specially designed measuring stand (Fig. 6) using the direct-injection tracer method. The tracers (red and blue ink) were injected into the flowing fluid (water) through small holes drilled in the bluff body, with their outlets located close to the vortex origins.

Using the fast camera, a series of pictures of the investigated phenomena were obtained. The camera allows the taking of a series of eight pictures with chosen intervals.



Fig. 6. Flow visualization measuring stand.

In the pictures obtained for circular cylinders acting as the bluff body (Fig. 7a), the markers are always visible. Therefore, it is obvious that the medium remains in this area or that its movement is strongly restricted. Finally, in the case of a circular cylinder, the stagnation region downstream of the bluff body is clearly visible. As is well-known, the circular cylinder does not ensure the generation of regular and strong vortices. In fact, the vortices are rather weak. Pictures obtained of the circular cylinder with a slit are presented in Fig. 7b. Intensive development of the vortices begins just after their origin. In this case, the

stagnation region is not an unmovable volume of fluid. The vortices, however, are easily distinguishable and remain strong over the entire distance downstream of the bluff body. Pictures obtained for a rectangular cylinder with a slit (Fig. 7c) are similar to those for a circular cylinder with a slit. In this case, the stagnation region is also strongly reduced. Conversely, the vortices created with the rectangular cylinder decay very early.

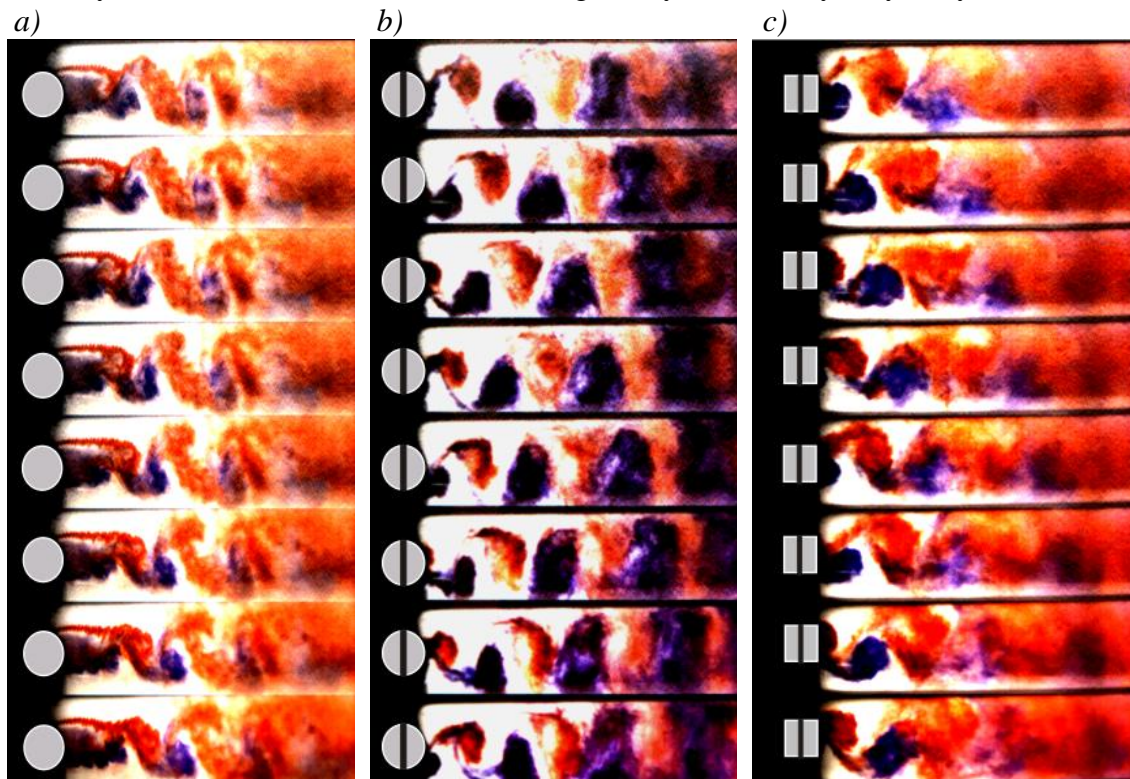


Fig. 7. Vortex generation on the bluff body: a – on a circular cylinder, b – on a circular cylinder with the slit, c – on a rectangular cylinder with the slit.

## 5.2. Hot-wire anemometry

In early designs of the vortex meter, hot-wire anemometry was applied as the eddy detector. However, its true advantages rely on the feasibility of the determination of the local velocity at the chosen point in the area where the vortices appear. Therefore, the use of a special module for hot-wire probe movement enables investigations of the entire area downstream of the bluff body.

The velocity distributions in the area downstream of the bluff body were determined on a measuring stand for gas meter calibration. The experiments were carried out for various bluff body shapes: a circular cylinder, a circular cylinder with a slit, a rectangular cylinder, a rectangular cylinder with a slit and a trapezoidal cylinder. The hot-wire probe, which had two wires, was moved along two axes perpendicular to the bluff body ( $x$  – towards the pipe wall and  $y$  – downstream of the bluff body). Therefore, the scanning of the whole flow velocity area was ensured. Two velocity components were calculated: transverse  $v_x$  and axial  $v_y$ . The investigations were carried out using a measuring stand for the calibration of gas flow meters. The results presented in Fig. 8-12 were obtained at a flow rate of 22 m<sup>3</sup>/h (the pipe diameter was equal to 40 mm).

Transverse velocity distributions obtained for various bluff body shapes differ considerably. Especially interesting are the differences in the closest neighborhood downstream of the bluff body.

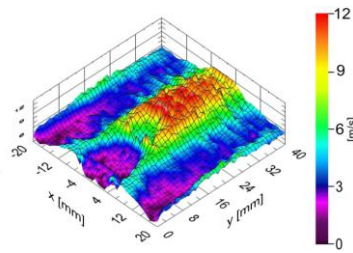


Fig. 8. Transverse velocity distribution for a circular cylinder.

In the case of the circular cylinder (Fig. 8), we can see the “classic” stagnation region, as in the Birkhoff model. At a considerable distance downstream of the bluff body, the transverse velocity is very low. As determined by investigations that are not described here, the axial velocity also decays in this area. Thus, a “dead zone” has been found. It can be concluded that fluid movement in this region decays. Only at a certain distance from the bluff body (approx. 1,5 d) does the velocity again increase.

The clear appearance of the stagnation region is also observed in the graphs obtained for the rectangular cylinder (Fig. 9) and the trapezoidal cylinder (Fig. 10). However, in the case of rectangular cylinder, the stagnation region is considerably shorter.

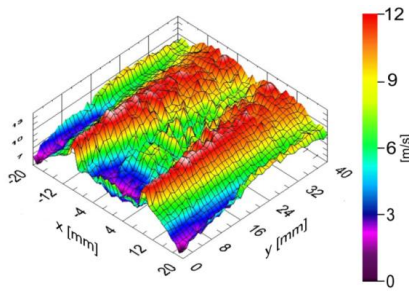


Fig. 9. Transverse velocity distribution for a rectangular cylinder.

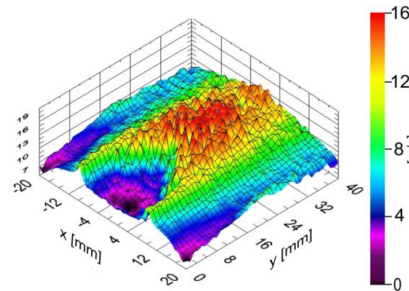


Fig. 10. Transverse velocity distribution for a trapezoidal cylinder.

Introduction of a slit to the bluff body caused radical changes in the flow velocity distributions (Figs. 11-12). This effect was found in all investigated bluff bodies. An especially strong effect occurred with the circular cylinder (Fig. 11). The stagnation region is entirely imperceptible. It is noteworthy that the vortex street is narrow and regular. Introduction of the slit into the rectangular cylinder also causes changes in the velocity distribution. The most interesting change is the considerable decrease of the size of the stagnation region. Experiments show that even the location of the slit influences the stagnation region size. A shorter distance from the upstream side results in more efficient reduction of the stagnation region.

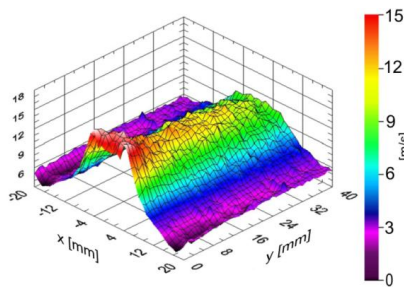


Fig. 11. Transverse velocity distribution for a circular cylinder with slit

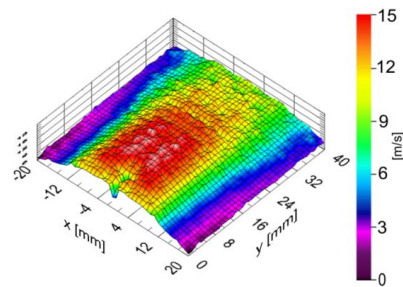


Fig. 12. Transverse velocity distribution for a rectangular cylinder with slit

For better recognition of the stagnation region properties, more detailed investigations have been carried out for the circular cylinder. The obtained results for various flow rates (Fig. 13) show that the length of the stagnation region depends on the flow rate. Furthermore, the distributions of transverse and axial velocity differ for both velocity components. The stagnation region may have a “tail” that performs pendulum-type motion. Once more, the actual phenomenon has proven to be much more complicated than the models indicate.

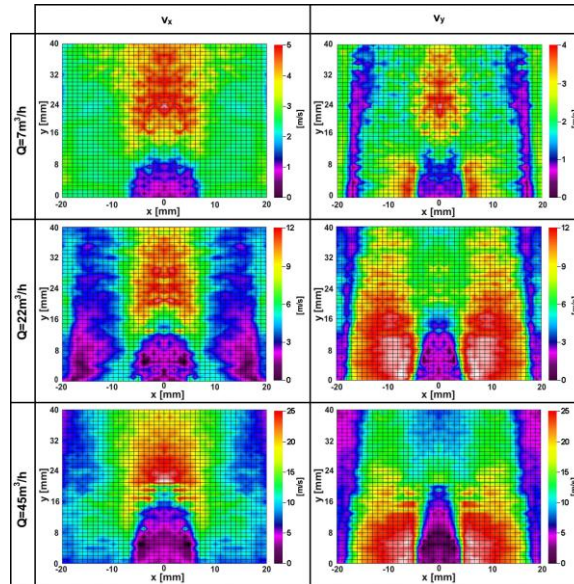


Fig. 13. Top view of velocity distributions for the circular cylinder ( $v_x$  – transverse velocity,  $v_y$  – axial velocity).

## 6. Conclusions

The stagnation region, already accounted for in Birkhoff’s model of vortex shedding, appears to play a very significant role in Karman vortex street development. Its push-pull motion constitutes an information channel that transfers “the message” of vortex generation to the other side of the bluff body. Therefore, the generation of the next vortex is initialized. This role is very important and determines the regular generation of vortices, alternating on both sides of the bluff body.

From the phenomenological model results, the length of the stagnation region strongly influences the rate of the vortex growth and increases the vortices’ rotation energy.

Laboratory investigations of the Karman vortex shedding phenomenon, using flow visualization and hot-wire anemometry, confirm the existence of a stagnation region.

Based on the flow visualization pictures, the existence of stagnation regions in the closest neighbourhood of the bluff body is clearly visible for the circular cylinder. The vortices form at the end of the stagnation region.

Results of hot-wire anemometry investigations also confirm the appearance of a stagnation region. Graphs obtained for the bluff bodies without the slit show that, in the closest neighbourhood downstream of the bluff body, an area of strongly reduced flow movement is noticeable.

The introduction of the slit into the bluff body strongly changes the picture of the phenomenon. This finding has been experimentally confirmed by both hot-wire anemometry and flow visualization investigations. The stagnation region becomes strongly reduced, which can be interpreted as a result of **the slit taking over the role of the stagnation region as an information channel for generating vortices**. Thus, in the bluff bodies with a slit, the stagnation region becomes unnecessary and decays.

In contrast, as results from the flow visualisation and from other laboratory investigations, the vortices generated on bluff bodies with a slit are stronger and more regular than those from solid bluff bodies. Therefore the conclusion that a reduction of the stagnation region is due to the introduction of a slit is beneficial from the point of view of vortex strength and regularity.

## Acknowledgments

This research project was supported by the Polish Ministry of Science and Higher Education (project No. 3600/B/T02/2009/36).

## Notes

$f$	–	<i>vortex shedding frequency</i>
$S_T$	–	<i>Strouhal number</i>
$d$	–	<i>bluff body diameter</i>
$v$	–	<i>flow velocity upstream the bluff body</i>
$\alpha$	–	<i>angle deviation of stagnation region</i>
$k_r$	–	<i>coefficient of restoring moment</i>
$\rho$	–	<i>fluid density</i>
$x$	–	<i>current vortex displacement from the bluff body axis</i>
$x_s$	–	<i>length of intensive development zone</i>
$x_k$	–	<i>length of intensive development and stabilization zones</i>
$D$	–	<i>pipe width</i>
$r$	–	<i>radius of the vortex</i>
$\omega$	–	<i>vortex angular velocity</i>
$v_{pc}$	–	<i>flow velocity 'driving' the vortex</i>
$v_{px}$	–	<i>current flow velocity at the distance <math>x</math> from the pipe axis</i>
$v_{p0}$	–	<i>flow velocity at the point of maximal fluid swelling</i>
$E_{rot}$	–	<i>rotation energy of the layer</i>
$m$	–	<i>mass</i>
$I$	–	<i>moment of inertia</i>
$k$	–	<i>layer number</i>
$\Delta z$	–	<i>width of the layer</i>
$E_{tot}$	–	<i>total rotation energy</i>
$\eta$	–	<i>dynamic viscosity</i>

## References

- [1] Pankanin, G.L. (2005). The Vortex Flowmeter: Various Methods of Investigating Phenomena. *Measurement Science and Technology*, (3), R1-R16 (Review article).
- [2] Cousins, T., Foster, S.A., Johnson, P.A. (1973). A linear and accurate flowmeter using vortex shedding. *Proc. Power Fluid for Process Control Symposium, Inst. Measurement and Control*, Guildford, UK, 45-46.
- [3] Miller, R.W., De Carlo, J.P., Cullen, J.T. (1977). A vortex flowmeter – calibration results and application experience. *Proc. Flow-Con*, Brighton, UK.
- [4] Lomas, D.J. (July/August 1975). Vortex flowmetering challenges the accepted techniques. *Control & Instrumentation*.

- [5] Turner, J.T., Popiel, C.O., Robinson, D.I. (1993). Evolution of an improved vortex generator. *Flow Measurement and Instrumentation*, 4, 249-259.
- [6] Igarashi, T. (13-17 August, 2000). Performance of new type vortex shedder for vortex flowmeter. *Proc. of Sixth Triennial International Symposium on Fluid Control, Measurement and Visualisation FLUCOME 2000*, Sherbrooke (Qc) Canada, 028.
- [7] Hans, V., Windorfer, H. (2003). Comparison of pressure and ultrasound measurements in vortex flowmeters, *Measurement*, 33, 121-133.
- [8] Menz, B. (1997). Vortex flowmeter with enhanced accuracy and reliability by means of sensor fusion and self-validation, *Measurement*, 22, 123-128.
- [9] Takahashi, S., Itoh, I. (1993). Intelligent vortex flowmeter. *Proc. of International Conference of Flow Measurement FLOMEKO 1993*, Seoul, Korea, 107-113.
- [10] Hans, V., Poppen, G. (1996). Measuring Vortex Frequencies using Undersampled Ultrasound Signals. *Proc. of International Conference of Flow Measurement FLOMEKO '96*, Beijing, China, 724-728.
- [11] Clarke, D.W. (2002). Designing phase-locked loops for instrumentation applications. *Measurement*, 32, 205-227.
- [12] Clarke, D.W., Ghaoud, T. (2003). A dual phase-locked loop for vortex flow metering. *Flow Measurement and Instrumentation*, 14, 1-11.
- [13] Huang, N.E., Shen, Z., Long, S.R., et al. (1998). The Empirical Mode Decomposition and The Hilbert Spectrum for Nonlinear and Non-stationary Time Series Analysis. *Proc. of the Royal Society of London*, 454, 903-995.
- [14] Sun, Z-Q., Zhou, J-M., Zhou, P. (2006). Application of Hilbert-Huang Transform to Denoising in Vortex Flowmeter. *J. Cent. South Univ. Technol.*, 13(5), 501-505.
- [15] Birkhoff, G. (1953). Formation vortex street. *Journal of Applied Physics*, 24(1), 98-103.
- [16] Birkhoff, G. (1957). Zaranonello E.H. Jets Wakes and Cavities, *Academic Press Inc.*, New York.
- [17] Funakawa, M. (1969). The Vibration of a Cylinder Caused by Wake Force in a Flow. *The Japan Society of Mechanical Engineers*, 12(53), 1003-1010.
- [18] Pankanin, G.L. (1994). Sensitivity of Vortex Meter Characteristics on Bluff Body Design. *Proc. of Fourth Triennial International Symposium on Fluid Control, Measurement and Visualisation FLUCOME'94*, Toulouse, France, 2, 893-898.
- [19] Cousins, T., Zanker, K. (1975). The performance and design of vortex meters. *Proc. Int Conf. On Flow Meters in the Mid 1970's*, NEL, East Kilbride, Scotland.
- [20] Pankanin, G.L., Berliński, J., Chmielewski, R. (2005). Analytical modelling of Karman vortex street. *Metrology and Measurement Systems*, 12(4), 411-425.
- [21] Pankanin, G.L., Berliński, J., Chmielewski, R. (2006). Simulation of Karman vortex street development using new model. *Metrology and Measurement Systems*, 13(1), 35-47.
- [22] Pankanin, G.L. (1-3 May, 2007). Experimental and Theoretical Investigations Concerning the Influence of Stagnation Region on Karman Vortex Shedding. *Proc. IMTC 2007, IEEE Instrumentation and Measurement Technology Conference*, Warsaw, Poland, CD-ROM proceedings.
- [23] Honda, S., Yamasaki, H. (1985). Vortex shedding in a three-dimensional flow through a circular pipe. *Proc. IMEKO X Congress*, Prague, Czech Republic, 139-149.
- [24] Igarashi, T. (2-6 September, 1985). Fluid flow around a bluff body used for a Karman vortex flowmeter. *Proc. of International Symposium on Fluid Control and Measurement FLUCOME TOKYO'85*, Tokyo, Japan, 1017-1022.
- [25] Pankanin, G., Kulińczak, A., Berliński, J. (2007). Investigations of Karman Vortex Street Using Flow Visualization and Image Processing. *Sensors and Actuators A: Physical*, 138, 366-375.
- [26] Pankanin, G.L., Kulińczak, A. (6-11 Sept., 2009). Determination of Vortex Convection Velocity with Application of Flow Visualization and Image Processing. *Proc. of XIX IMEKO World Congress 'Fundamental and Applied Metrology'*, Lisbon, Portugal.